Journal of Power Sources 195 (2010) 7426–7431

Contents lists available at ScienceDirect

Journal of Power Sources

journal homepage: www.elsevier.com/locate/jpowsour

A mixture of triethylphosphate and ethylene carbonate as a safe additive for ionic liquid-based electrolytes of lithium ion batteries

Boor Singh Lalia, Nobuko Yoshimoto, Minato Egashira, Masayuki Morita*

Graduate School of Science and Engineering, Yamaguchi University, 2-16-1 Tokiwadai, Ube 755-8611, Japan

ARTICLE INFO

Article history:
Received 17 April 2010
Received in revised form 22 May 2010
Accepted 25 May 2010
Available online 1 June 2010

Keywords:
Triethylphosphate
Ethylene carbonate
Ionic liquid
Conductivity
Lithium-ion batteries

ABSTRACT

A binary mixture of triethylphosphate (TEP) and ethylene carbonate (EC) has been examined as a new non-flammable additive for ionic liquid-based electrolytes for lithium-ion batteries. The optimized electrolyte composition consists of 0.6 mol dm^{-3} (=M) LiTFSI in PP13TFSI mixed with TEP and EC in volume ratio of 80:10:10, where TFSI and PP13 denote bis(trifluoromethanesulfonyl)imide and *N*-methyl-*N*-propylpiperidinium, respectively. The ionic conductivity of PP13TFSI dissolving 0.4 M LiTFSI was improved from 8.2×10^{-4} S cm^{-1} to 3.5×10^{-3} S cm^{-1} (at 20 °C) with the addition of TEP and EC. The electrochemical behavior of 0.4 M LiTFSI/PP13TFSI with and without TEP and EC was studied by cyclic voltammetry, which showed no deteriorating effect by the addition of TEP and EC on the electrochemical window of PP13TFSI. The flammability of the electrolyte was tested by a direct flame test. The proposed ionic liquid-based electrolyte revealed significant improvements in the electrochemical charge–discharge characteristics for both graphite negative and $LiMn_2O_4$ positive electrodes.

1. Introduction

Considerable attention has been drawn to room temperature ionic liquids (RTILs) as "green" alternative solvents to traditional organic solvents used in lithium-ion batteries (LIBs) [1–6]. They have substantial potential as solvents due to their unique properties, such as non-flammable, non-volatile, thermally stable, wide liquidus range and relatively wide electrochemical window [7–10]. These properties make RTILs as attractive candidates for the electrolyte of a safer LIB. The RTILs generally consist of organic cations like alkylimidazolium, alkylpyridinium, alklypyrolidinium, alkylpyrazolium, quaternary ammonium, etc. [11–15], and large size of inorganic or organic anions, such as tetrafluoroborate (BF_4^-), hexafluorophosphate (PF_6^-), trifluoromethanesulfonate (Tf^-), and bis(trifluoromethanesulfonyl)imide ($TFSI^-$). Thus, the physical and chemical properties of RTIL can be tuned by a combination of cation and anion.

Alkylimidazolium based ionic liquids have been widely studied due to their low viscosity and high ionic conductivity. But the most of them are suffered from poor cathodic stability and cannot be used for graphite/lithium metal anode [16]. Among RTILs, imide salts of quaternary alkylammonium and alkylpyridinium are of particular interest due to their wide electrochemical window and cathodic stability [17,18]. These ionic liquids showed excellent properties in a $Li/LiCoO_2$ cell system. However, they are highly viscous and have low ionic conductivity. The electrolytes having high ionic conductivity are desirable for high power-density applications such as electric vehicles (EVs) and hybrid electric vehicles (HEVs). Some efforts have been made to improve the performance of ionic liquid-based electrolytes by addition of organic solvents like ethylene carbonate (EC), dimethylcabonate (DMC), ethylmethyl carbonate (EMC), vinylenecarbonate (VC), etc. [19–22]. The addition of flammable organic solvents, however, affects the flammability and thermal properties of the resulting electrolytes. From the viewpoint of the safety of LIBs, there needs to look for non-flammable additive for ionic liquid-based electrolytes to realize a safe battery system. Alkylphosphates have been used as fire retardant co-solvents in organic solution electrolytes [23–25]. The addition of alkylphosphates effectively suppresses the flammability of the organic electrolytes. In the previous work, we reported that trimethylphosphate (TMP) and triethylphosphate (TEP) can be used as the fire retardant components in novel non-flammable organic electrolyte systems [26,27].

In the present paper, a binary mixture of TEP and EC has been proposed as a non-flammable additive for electrolytes based on an ionic liquid, *N*-methyl-*N*-propylpiperidinium bis(trifluoromethanesulfonyl)imide (PP13TFSI). TEP has low viscosity, low melting point, high boiling point, non-flammability and relatively high dielectric constant. These properties are useful to improve the ionic conductivity, viscosity, thermal stability and operational temperature range of the PP13TFSI-based electrolyte. On the other hand, EC component would contribute to

* Corresponding author. Tel.: +81 836 85 9211; fax: +81 836 85 9201.
E-mail address: morita@yamaguchi-u.ac.jp (M. Morita).

0378-7753/$ – see front matter © 2010 Elsevier B.V. All rights reserved.
doi:10.1016/j.jpowsour.2010.05.040

form good interface between a graphite-based negative electrode and liquid electrolyte. The effects of addition of EC and TEP on the ionic conductivity, electrochemical stability, interfacial properties and thermal stability of PP13TFSI dissolving lithium salt (LiTFSI/PP13TFSI) have been investigated.

2. Experimental

PP13TFSI (Kanto Reagent), LiTFSI (Aldrich), EC (Kishida Chemical; Battery grade) and TEP (Wako Chemical) were used as received due to their high purity and low water contamination. The liquid electrolyte was prepared by dissolving 0.4 M LiTFSI in PP13TFSI. The mixed electrolytes were prepared by adding appropriate amount of LiTFSI in PP13TFSI, EC and TEP under an Ar atmosphere. A direct flame test was carried out to examine the flammability of the binary mixture of TEP and EC, and the electrolyte containing PP13TFSI, TEP and EC. A piece of glass filter paper impregnated with the test solution was set at 30 mm above the flame of Bunsen burner. The ignition time after flame setting and the self-extinguish time after removing the burner flame were measured as indices of the nonflammability.

The ionic conductivity of the electrolytes was measured by an ac impedance method in a frequency range from 100 kHz to 1 Hz using a frequency response analyzer controlled by a personal computer. The interfacial properties were examined by means of a symmetric cell, Li/electrolyte/Li, using Li foil disks (14 mm diameter) as the active electrode material. The electrochemical stability of the electrolyte was measured at a glassy carbon (GC: GC-30, Tokai Carbon) or a synthetic graphite (TIMREX KS6, TIMCAL) electrode by cyclic voltammetry (CV) using a three-electrode cell with Li foil counter and reference electrodes. The potential scan rates in these experiments were 1 mV s^{-1} for GC and 0.1 mV s^{-1} for the graphite electrode.

Charge–discharge cycling tests were conducted using a CR2036 coin-type two-electrode cell with the graphite or $LiMn_2O_4$ (Toda Kogyo) working electrode and a Li foil counter electrode. A sheet of glass microfiber filter paper (Whatman, Grade GF/A, pore size 1.6 μm) was used as the separator. The negative electrode was prepared from a slurry containing 96 mass% active material (KS6) with 4 mass% poly(vinylidene fluoride) (PVdF) binder and 1-methylpyrrolydine-2-on (NMP) solvent. The size of the negative electrode was 13 mm in diameter and the average active material loading was 1.7 mg cm^{-2}. Charge–discharge curves were measured in the voltage range of 0.01–2.0 V. In this paper, the term "charge" for the test cell using graphite working electrode denotes the cathodic reduction of the graphite working electrode and the term "discharge" is used for the anodic oxidation of the lithiated graphite electrode. The cell was first charged at *C*/3 current rate to 0.01 V and then charged at constant voltage of 0.01 V for 3 h. The discharge was carried out under a constant current rate of 1*C* or *C*/5.

With respect to the examination in the positive electrode side, the working electrode was prepared by coating slurry containing 80 mass% of the active material $LiMn_2O_4$, 10 mass% of acetylene black as a conductive reagent, and 10 mass% of PVdF binder in NMP solvent. The working electrode having 13 mm in diameter and the active mass loading of 2.3 mg cm^{-2} was punched from the electrode sheet. The counter electrode was a Li foil disk with 15 mm in diameter. The cell was charged to the cut-off voltage of 4.6 V at *C*/2 rate and then discharged to 3.5 V at 1*C* or 3*C* current rate, where we employed rather high cut-off voltage for charging because of the two-electrode cell using Li metal counter electrode. These electrochemical measurements were carried out at room temperature (23 ± 2 °C) under a dry Ar atmosphere.

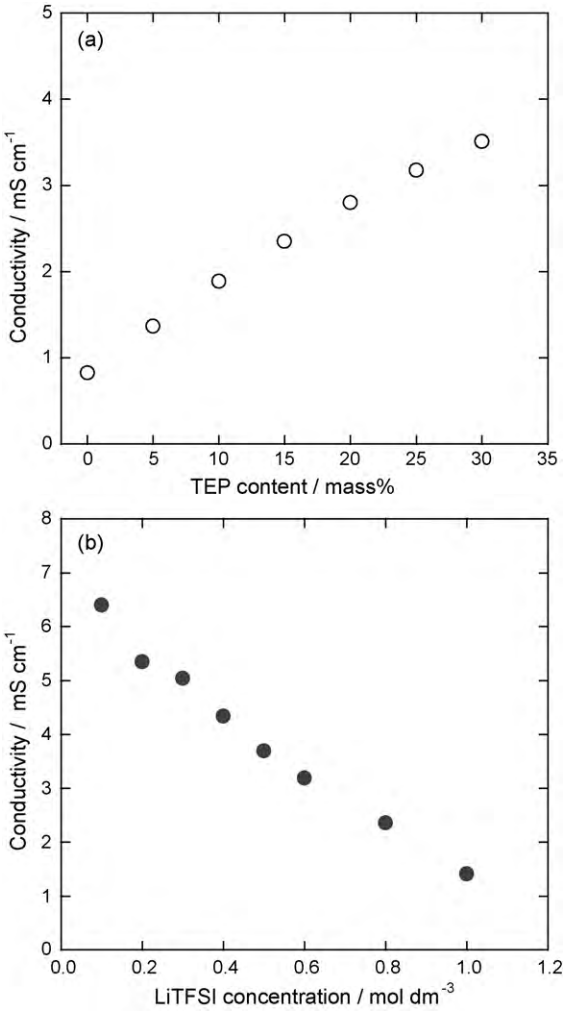

Fig. 1. Ionic conductivity of (a) 0.4 M LiTFSI/PP13TFSI + TEP as a function of TEP content and (b) LiTFSI/PP13TFSI + TEP + EC (80:10:10) as a function of LiTFSI concentration.

3. Results and discussion

Fig. 1a shows the variation in the ionic conductivity of 0.4 M LiTFSI/PP13TFSI with the addition of 0–30 mass% of TEP at 20 °C. The addition of 30 mass% TEP led to increase in the conductivity of 0.4 M LiTFSI/PP13TFSI from 8.2×10^{-4} S cm^{-1} to 3.5×10^{-3} S cm^{-1}. The conductivity variation of LiTFSI/PP13TFSI + TEP + EC (80:10:10) with the content of LiTFSI is given in Fig. 1b. With the increase in the LiTFSI concentration in the ternary mixture of PP13TSI, TEP and EC, the ionic conductivity of the solution electrolyte decreases. This may be due to an increase in the viscosity of the electrolyte with addition of the Li salt, which decreases the mobility of whole ions in the system. The major ionic species for charge transportation will be the ionic liquid cation and anion, while the mobility of Li^+ is also influenced by the viscosity of the electrolyte system. Some important properties of PP13TFSI, TEP and EC are given in Table 1. The base

Table 1
Selected physico-chemical properties of the solvents.

	Viscosity (η), mPa s	Melting point, °C	Dielectric constant (ε_r)	Density (ρ), 10^3 kg m^{-3}
PP13TFSI	151	12	–	1.43
EC	1.9[a]	38	91.2[a]	1.32
TEP	1.6	−56	13.1	1.07

[a] At 40 °C.

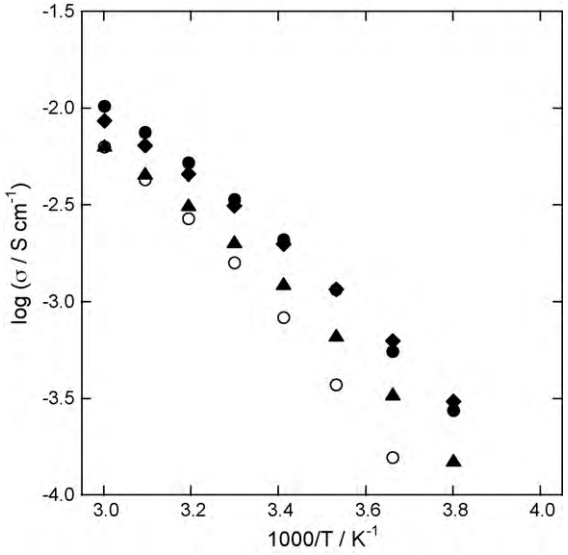

Fig. 2. Temperature dependences of the ionic conductivity for 0.4 M LiTFSI/PP13TFSI (○), 0.6 M LiTFSI/PP13TFSI + TEP (80:20) (▲), 0.6 M LiTFSI/PP13TFSI + TEP (70:30) (♦) and 0.6 M LiTFSI/PP13TFSI + TEP + EC (80:10:10) (●).

ionic liquid (PP13TFSI) used for the liquid electrolyte containing Li salt has high viscosity (η = 151 mPa s). The addition TEP with low viscosity and low melting point (η = 1.6 mPa s and M.P. = −56 °C) results in the decrease in the viscosity of the electrolyte system. Thus, two factors would contribute to the increase in conductivity of the ionic liquid-based electrolyte; reasonably high dielectric constant and low viscosity of TEP. The lowering in viscosity of the electrolyte with the addition of TEP in 0.4 M LiTFSI/PP13TFSI facilitates the mobility of the ions and reasonably high dielectric constant of TEP assists the dissociation of LiTFSI in PP13TFSI, and hence resulted in the increase of the conductivity of the system. The temperature dependences of the ionic conductivity of the electrolytes containing LiTFSI in binary mixture of PP13TFSI + TEP, and in ternary mixture of PP13TFSI + TEP + EC for the temperature range from −10 °C to 60 °C are shown in Fig. 2. The conductivity increases with the increase in temperature and shows a curvature, which is characteristics of a glassy liquid and follows the VTF behavior, expressed by following equation,

$$\sigma = \sigma_o \exp\left(\frac{-B}{T - T_o}\right) \quad (1)$$

where σ_o (S cm^{-1}), B (K) and T_o (K) are constants. The best-fit parameters were calculated and are listed in Table 2. The electrolyte with composition of 0.6 M LiTFSI/PP13TFSI + TEP + EC (80:10:10) has conductivity comparable to 0.6 M LiTFSI/PP13TFSI + TEP (70:30), and hence selected for the further studies.

As the results of the direct flame test for the binary mixture of TEP and EC, and the electrolyte containing PP13TFSI, TEP and EC, 30 vol% of TEP was the minimum amount to suppress the flammability of the EC solvent. That is, EC containing 30 vol% TEP or more did not ignite, and the ionic liquid electrolytes containing TEP + EC as the additive whose volume ratio was higher than 1/3 showed no ignition. However, we use equal volume ratio of TEP and EC as the additive, eg. 0.6 M LiTFSI/PP13TFSI + TEP + EC (80:10:10), being completely non-flammable in nature, for the high safety of the electrolyte system.

Table 2
VTF parameters for the temperature dependence of ionic conductivity.

Electrolyte system	σ_o, S cm^{-1}	B, 10^2 K	T_o, K	R^2
0.4 M LiTFSI/PP13TFSI	1.39	3.89	179	0.99
0.6 M LiTFSI/PP13TFSI + TEP (80:20)	1.24	4.16	160	0.99
0.6 M LiTFSI/PP13TFSI + TEP (70:30)	1.05	3.63	161	0.99
0.6 M LiTFSI/PP13TFSI + TEP + EC (80:10:10)	1.51	4.19	158	0.99

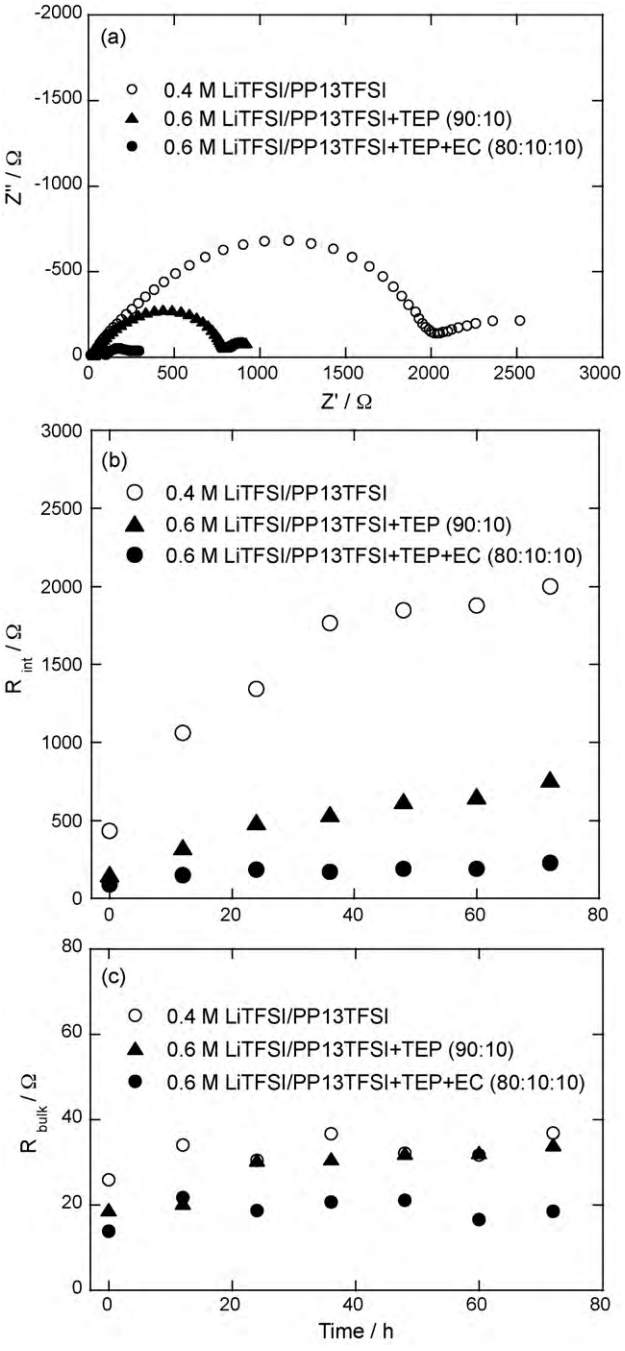

Fig. 3. Ac impedance results for an Li/electrolyte/Li symmetric cell. (a) Nyquist plots for cells with different electrolytes, (b) variation in the interfacial resistance (R_{int}) with time, and (c) variation in the bulk resistance (R_{bulk}) with time.

Electrochemical impedance spectroscopy was used to investigate the effects of addition of TEP and EC on the interfacial/bulk resistance of an Li/electrolyte/Li symmetric cell. The impedance spectra were recorded for the cell for 72 h after a constant interval of 12 h in 0.01 Hz to 20 kHz frequency range. The electrolytes used were 0.4 M LiTFSI/PP13TFSI, 0.6 M LiTFSI/PP13TFSI + TEP (90:10) and 0.6 M LiTFSI/PP13TFSI + TEP + EC (80:10:10). Fig. 3a shows the typical Nyquist plots for the systems after 72 h. The high frequency intercept of the semicircle is generally considered as the bulk resistance of electrolyte (R_{bulk}) and low frequency intercept as the

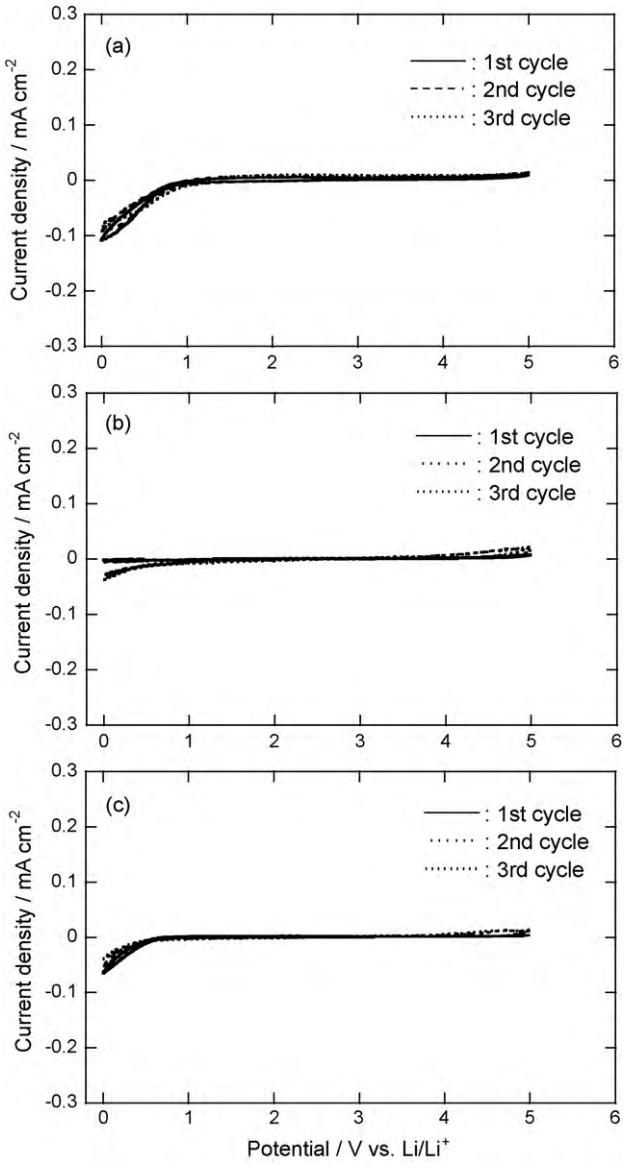

Fig. 4. Cyclic voltammograms for GC electrode in (a) 0.4 M LiTFSI/PP13TFSI, (b) 0.6 M LiTFSI/PP13TFSI + TEP (80:20), and (c) 0.6 M LiTFSI/PP13TFSI + TEP + EC (80:10:10). Scan rate: 1 mV s^{-1}.

electrode/electrolyte interface resistance (R_{int}). Fig. 3b shows the variations in R_{int} with duration time for the symmetrical cells using different electrolyte compositions. The interfacial resistance of the Li/electrolyte interface increased with time for the cell using 0.4 M LiTFSI/PP13TFSI electrolyte. For 0.6 M LiTFSI/PP13TFSI + TEP (80:20) and 0.6 M LiTFSI/PP13TFSI + TEP + EC (80:10:10) electrolytes, however, smaller interfacial resistances were observed, and they did not increase significantly with time. These results reveal that a good interface was developed between metallic lithium and the electrolyte with the addition of TEP and EC. Fig. 3c indicates the change in the bulk resistance with time for the electrolyte with and without the additive components. The addition of TEP and EC reduces the bulk resistance of the electrolyte: 0.4 M LiTFSI/PP13TFSI, which is well consistent with the conductivity results as shown in Fig. 2. The variation in R_{bulk} with the storage time was also rather small in the system containing TEP and EC, compared with the others.

The effects of the addition of TEP and EC on the electrochemical window of the base electrolyte, 0.4 M LiTFSI/PP13TFSI, were investigated using cyclic voltammetry. Fig. 4 shows typical

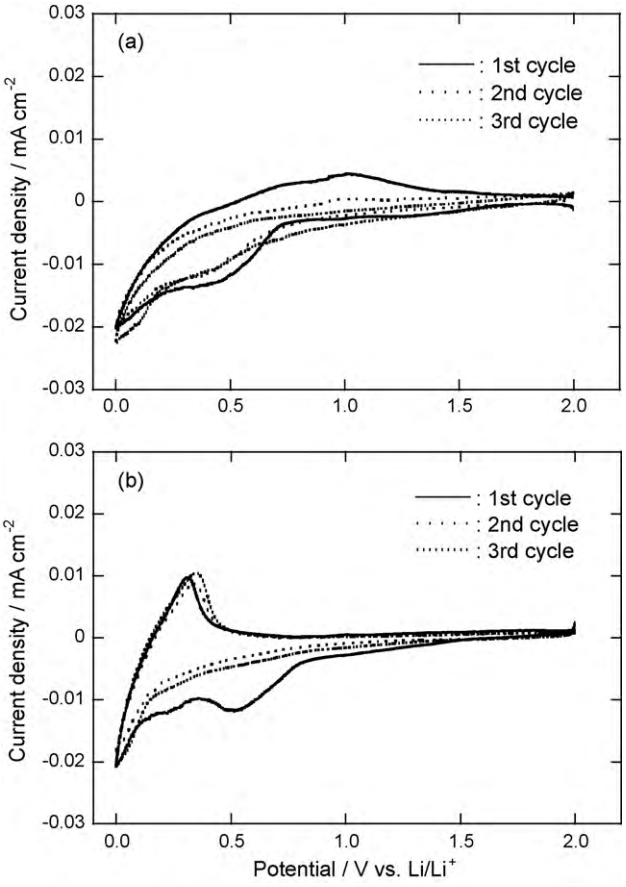

Fig. 5. Cyclic voltammograms for graphite (KS-6) in (a) 0.4 M LiTFSI/PP13TFSI and (b) 0.6 M LiTFSI/PP13TFSI + TEP + EC (80:10:10). Scan rate: 0.1 mV s^{-1}.

voltammograms for the electrolytes, 0.4 M LiTFSI/PP13TFSI, 0.6 M LiTFSI/PP13TFSI + TEP (80:20) and 0.6 M LiTFSI/PP13TFSI + TEP + EC (80:10:10), which were recorded at ambient temperature in the potential range of 0–5.0 V vs. Li/Li$^+$ at a scan rate of 1.0 mV s^{-1}. There is no oxidation current observed up to 5.0 V for 0.4 M LiTFSI/PP13TFSI electrolyte (Fig. 4a). In the cathodic scan, however, reductive current was observed in 0.9–0 V, which may be due to cathodic decomposition of the electrolyte on GC. The addition of TEP and EC in the base electrolyte (0.4 M LiTFSI/PP13TFSI) reduces the reductive current as shown in Fig. 4b and c. These results indicate that the binary mixture of TEP and EC is useful to suppress the cathodic reduction of the electrolyte on GC in the negative potential ranges, and does not adversely affect the electrochemical window of the base electrolyte.

The voltammetric responses of graphite (KS-6) electrode in 0.4 M LiTFSI/PP13TFSI and 0.6 M LiTFSI/PP13TFSI + TEP + EC (80:10:10) are shown in Fig. 5, where lower potential scan rate of 0.1 mV s^{-1} was employed. In the cathodic scan for base electrolyte (Fig. 5a), two reduction peaks observed at ~0.7 V and ~0.2 V vs. Li/Li$^+$ are probably due to intercalation of PP13$^+$ and Li$^+$ ions in the graphite, respectively. In the reverse (anodic) scan from 0 V to 2 V, two broad oxidation peaks were observed, which would relate with de-intercalation of those species form the electrode. However, the current density faded for the repeated cycles, which may be due to formation of highly resistive layer on the electrode surface. Fig. 5b shows the cyclic voltammograms for graphite in the additive containing electrolyte, 0.6 M LiTFSI/PP13TFSI + TEP + EC (80:10:10). During the first cathodic scan, an irreversible reduction current peak was observed at about 0.9 V, which corresponds to the cathodic decomposition of EC on the graphite surface to form

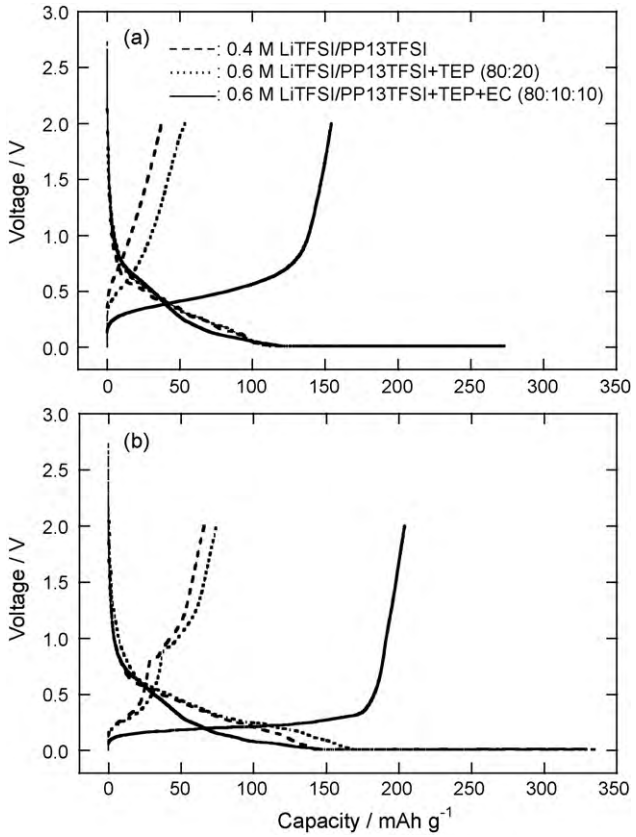

Fig. 6. First charge–discharge curves for graphite (KS6) negative electrode with different electrolyte systems at (a) 1*C* and (b) *C*/5 discharge rates.

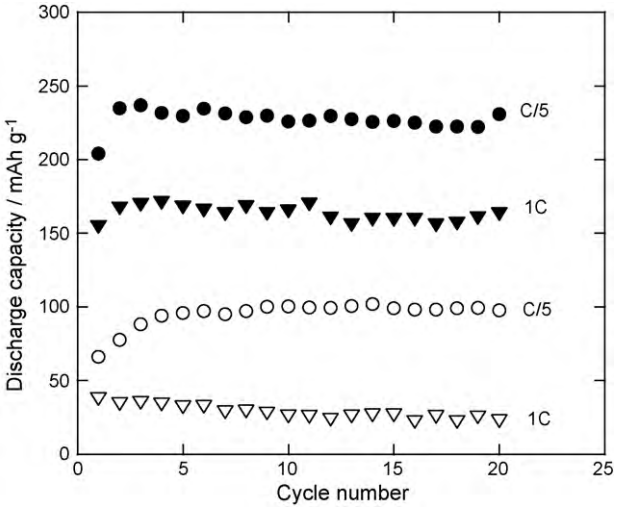

Fig. 7. Cycle performances of graphite (KS-6) negative electrode in 0.4 M LiTFSI/PP13TFSI (○, ▽) and 0.6 M LiTFSI/PP13TFSI + TEP + EC (80:10:10) (●, ▼).

so-called "solid electrolyte interphase" (SEI). The electrochemical intercalation of Li^+ was observed at ca. 0.2 V. During the reverse scan, a sharp current peak corresponding to the de-intercalation of lithium from the electrode was detected. For the following cycles, sharp redox current peaks were observed without significant fading of the current density. These results reveal that the addition of TEP and EC effectively improves the performance of the ionic liquid-based electrolyte for graphite negative electrode.

Charge–discharge curves of the graphite/Li half cell using the electrolyte with and without the additives are shown in Fig. 6. The half cell was galvanostatically charged (Li-intercalation) at *C*/3 rate and discharged (de-intercalation of Li^+) at two different current values, 1*C* and *C*/5 rates. The addition of TEP and EC improved the discharge capacity from 37.5 mAh g^{-1} to 154.2 mAh g^{-1} at 1*C* discharge rate (Fig. 6a) and 66.1 mAh g^{-1} to 204.1 mAh g^{-1} at *C*/5 rate (Fig. 6b). The increment in discharge capacity is due to lowering in viscosity of the electrolyte with the addition of TEP and EC, which would assist to enhance the wettability of the electrode and the mobility of Li^+ at the electrode/electrolyte interface. The cyclic performances of the graphite/Li half cell using modified and unmodified electrolyte systems are presented in Fig. 7. A good cycleability was observed at both discharge rates of 1*C* and *C*/5. However, the value of the discharge capacity was still lower than the ideal capacity of the present negative electrode material (ca. 350 mAh g^{-1}). This is probably due to insufficient interface conditions for the present cell construction.

Fig. 8 indicates the first charge–discharge curves for $LiMn_2O_4$ positive electrode (Li/$LiMn_2O_4$ half cell) in different electrolyte systems of 0.4 M LiTFSI/PP13TFSI, 0.6 M LiTFSI/PP13TFSI + TEP (80:20) and 0.6 M LiTFSI/PP13TFSI + TEP + EC (80:10:10) under different *C* rates. We have found that the positive electrode with the modified electrolyte containing TEP and EC has sufficiently high discharge capacity of 99.1 mAh g^{-1} and 64.2 mAh g^{-1} even at high discharge rates at 1*C* and 3*C*, respectively. The cycle performances of $LiMn_2O_4$ positive electrode were examined in 0.4 M LiTFSI/PP13TFSI and 0.6 M LiTFSI/PP13TFSI + TEP + EC (80:10:10) for 20 cycles, and their results are given in Fig. 9. There is no capacity fading with the cycle for the modified electrolyte at 1*C* discharge rate, whereas a small capacity fading was observed during the initial 5 cycles at 3*C* discharge rate.

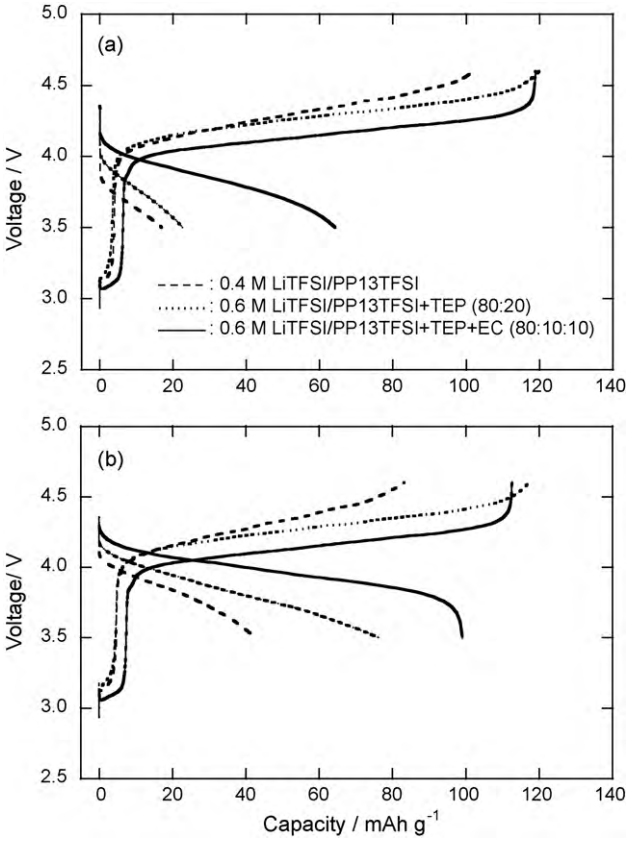

Fig. 8. First charge–discharge curves for $LiMn_2O_4$ positive electrode with different electrolyte systems at (a) 3*C* and (b) 1*C* discharge rates.

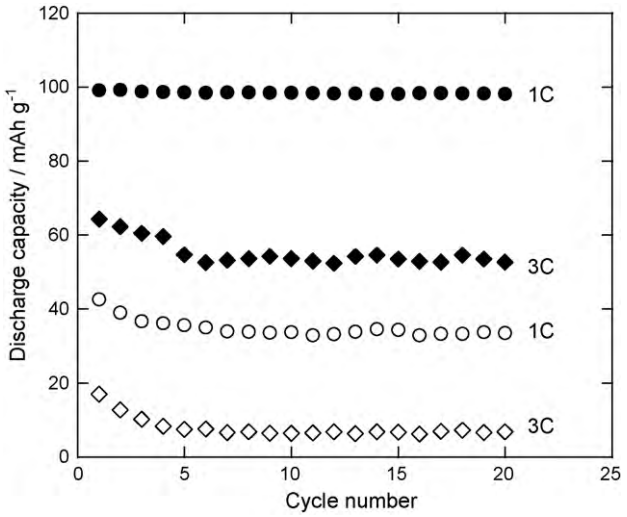

Fig. 9. Cycle performances of $LiMn_2O_4$ positive electrode in 0.4 M LiTFSI/PP13TFSI (○, ◊) and 0.6 M LiTFSI/PP13TFSI + TEP + EC (80:10:10) (●, ♦).

Nyquist plots of the ac impedance measured for Li/$LiMn_2O_4$ cells with different electrolyte compositions are shown in Fig. 10. The impedance was measured after charging the cell up to 4.6 V. Each plot consists of two flat semicircles. As the test cell consisted of two electrodes, $LiMn_2O_4$ positive and Li metal negative electrodes, these two semicircles respectively correspond to two equivalent circuits at Li/electrolyte and $LiMn_2O_4$/electrolyte interface. The addition of TEP and EC in the liquid electrolyte significantly reduced the size of the semicircle, especially at lower frequency region. Judging from the differences in the time constant for the process at two interfaces, the equivalent circuit in the lower frequency region would be attributed to the process at the positive electrode side. Thus, the additive components, TEP and EC, are effective to reduce the interfacial resistances, especially at the oxide electrode side, as also shown in Fig. 4c. We consider that there is some difference in the chemistry at the interface, so-called SEI formation, depending on the electrolyte composition. Such a change in the interfacial property would reduce the interfacial impedance and then improve the charge–discharge performance of the cell. These results obtained in above experiments reveal that TEP and EC are safe and effective components for ionic liquid-based electrolyte that improve the electrochemical performances of graphite/$LiMn_2O_4$ battery system.

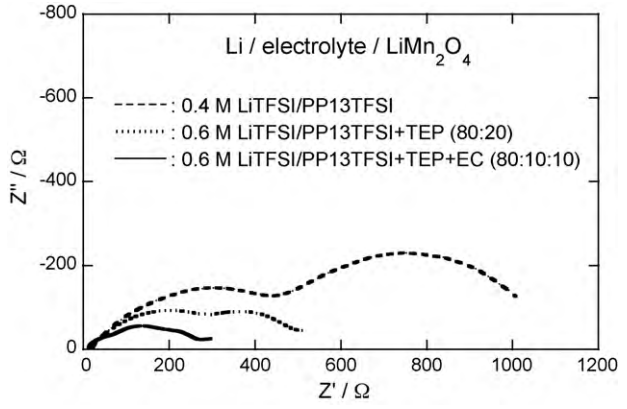

Fig. 10. Nyquist plots of ac impedance for Li/$LiMn_2O_4$ cells with different electrolyte systems.

4. Conclusions

The addition of binary mixture of TEP and EC in 0.4 M LiTFSI/PP13TFSI improves the ionic conductivity, electrochemical performances and safety of the graphite/$LiMn_2O_4$ battery system. The charge–discharge cycle tests indicated that TEP has no deteriorating effect on the electrochemical window of the base electrolyte. Even the addition of TEP improves the cathodic stability of the electrolyte. The interfacial resistance of the Li/electrolyte interface remains unchanged with the addition of TEP and EC which suggests the good compatibility of the additives with the metallic Li surface. The present results strongly suggest that TEP and EC can be used as a safe additive for LIB system using $LiMn_2O_4$ positive electrode.

Acknowledgement

This work was financially supported by a program of "Development of High-performance Battery System for Next-generation Vehicles" (Li-EAD) from the New Energy and Industrial Technology Development Organization (NEDO) of Japan.

References

[1] M. Lipsztajn, R.A. Osteryoung, Inorganic Chemistry 24 (1985) 716.
[2] J. Fuller, R.T. Carlin, R.A. Osteryoung, Journal of Electrochemical Society 144 (1997) 3881.
[3] Y.S. Fung, R.Q. Zhou, Journal of Power Sources 81–82 (1999) 891.
[4] H. Sakaebe, H. Matsumoto, Electrochemistry Communications 5 (2003) 594.
[5] B. Garcia, S. Lavallee, G. Perron, C. Michot, M. Armand, Electrochimica Acta 49 (2004) 458.
[6] P.C. Howlett, D.R. MacFarlane, A.F. Hollenkamp, Electrochemical and Solid-State Letters 7 (2004) A97.
[7] P. Bonhote, A.-P. Dias, N. Papageorgiou, K. Kalyanasundaram, M. Gratzel, Inorganic Chemistry 35 (1996) 1168.
[8] A. Noda, K. Hayamizu, M. Watanabe, Journal of Physical Chemistry B 105 (2001) 460.
[9] A. Webber, G.E. Blomgren, in: W.A.V. Schalkwijk, B. Scrosati (Eds.), Advances in Lithium-Ion Batteries, Kluwer Academic/Plenum, New York, 2002, p. 185.
[10] H. Ohno, M. Yoshizawa, Solid State Ionics 154–155 (2002) 303.
[11] J.S. Wilkes, J.A. Levisky, R.A. Wilson, C.L. Hussey, Inorganic Chemistry 21 (1982) 1263.
[12] D.R. MacFarlane, P. Meakin, J. Sun, N. Amini, M. Forsyth, Journal of Physical Chemistry B 103 (1999) 4164.
[13] G.J.C. Mamantov, T.D.J. Dunstan, Electrochemical Systems Inc., US patent 5,552,241 (1996).
[14] C. Arbizzani, F. Soavi, M. Mastragostino, Journal of Power Sources 162 (2006) 735.
[15] M. Freemantle, Chemical and Engineering News 13 (1998) 32.
[16] M. Ishikawa, T. Sugimoto, M. Kikuta, E. Ishiko, M. Kono, Journal of Power Sources 162 (2006) 658.
[17] Y. Katayama, M. Yukumoto, T. Miura, Electrochemical and Solid-State Letters 6 (2003) A96.
[18] H. Sakaebe, H. Matsumoto, K. Tatsumi, Journal of Power Sources 146 (2005) 693.
[19] T. Sato, T. Maruo, S. Marukane, K. Takagi, Journal of Power Sources 138 (2004) 253.
[20] H. Zheng, K. Jiang, T. Abe, Z. Ogumi, Carbon 44 (2006) 203.
[21] J. Xu, J. Yang, Y. NuLi, J. Wang, Z. Zhang, Journal of Power Sources 160 (2006) 621.
[22] A. Guerfi, M. Dontigny, P. Charest, M. Petitclerc, M. Lagacé, A. Vijh, K. Zaghib, Journal of Power Sources 195 (2010) 845.
[23] X.M. Wang, E. Yasukawa, S. Kasuya, Journal of Electrochemical Society 148 (2001) A1058.
[24] Y.E. Hyung, D.R. Vissers, K. Amine, Journal of Power Sources 119–121 (2003) 383.
[25] .F. Xiang, Q.Y. Jin, C.H. Chen, X.W. Ge, S. Guo, J.H. Sun, Journal of Power Sources 174 (2007) 335.
[26] N. Yoshimoto, Y. Niida, M. Egashira, M. Morita, Journal of Power Sources 163 (2006) 238.
[27] B.S. Lalia, T. Fujita, N. Yohimoto, M. Egashira, M. Morita, Journal of Power Sources 186 (2009) 211.